Simulating Sediment Transport in a Flume with Forced Pool-Riffle Morphology: Examinations of Two One-Dimensional Numerical Models

Yantao Cui[1]; John K. Wooster[2]; Jeremy G. Venditti[3]; Scott R. Dusterhoff[4]; William E. Dietrich[5]; and Leonard S. Sklar[6]

Abstract: One-dimensional numerical sediment transport models (DREAM-1 and DREAM-2) are used to simulate seven experimental runs designed to examine sediment pulse dynamics in a physical model of forced pool-riffle morphology. Comparisons with measured data indicate that DREAM-1 and -2 closely reproduce the sediment transport flux and channel bed adjustments following the introduction of fine and coarse sediment pulses, respectively. The cumulative sediment transport at the flume exit in a DREAM-1 simulation is within 10% of the measured values, and cumulative sediment transport at flume exit in a DREAM-2 simulation is within a factor of 2 of the measured values. Comparison of simulated and measured reach-averaged aggradation and degradation indicates that 84% of DREAM-1 simulation results have errors less than 3.3 mm, which is approximately 77% of the bed material geometric mean grain size or 3.7% of the average water depth. A similar reach-averaged comparison indicates that 84% of DREAM-2 simulation results have errors less than 7.0 mm, which is approximately 1.7 times the bed material geometric mean grain size or 11% of the average water depth. Simulations using measured thalweg profiles as the input for the initial model profile produced results with larger errors and unrealistic aggradation and degradation patterns, demonstrating that one-dimensional numerical sediment transport models need to be applied on a reach-averaged basis.

DOI: 10.1061/(ASCE)0733-9429(2008)134:7(892)

CE Database subject headings: Sediment transport; Numerical models; Movable bed models; Channel morphology; Simulation.

Introduction

One-dimensional (1D) numerical sediment transport models have been widely used, and their applications have helped engineers and fluvial geomorphologists attack many practical problems and research questions. Implicit in their formulation, 1D numerical sediment transport models are not capable of simulating detailed local topographic features such as pools and riffles in rivers for the following reasons: (a) 1D models simplify the governing equations of mass and momentum conservation by ignoring the lateral component of the velocity, shear stress, and sediment flux vectors (and vertical component of the velocity vector); and (b) parameters retained in governing equations (e.g., water depth, streamwise flow velocity, streamwise shear stress, bed elevation, and grain size distribution) are averaged across channel cross sections (and vertically through the water column for flow parameters). For example, pools in rivers often form due to strong secondary flow and flow accelerations associated with channel curvature that are not accounted for within a 1D numerical sediment transport model. Thus, the majority of local hydraulics of pools associated with channel curvature will not be captured in a 1D numerical model simulation. Although the reach-averaged nature (i.e., the inability to predict detailed topographic features) of 1D sediment transport modeling may be inferred to some extent in many practical applications, in many cases it is not explicitly adhered to when applying models.

In this paper, we use two 1D numerical sediment transport models to simulate channel aggradation and degradation due to variations in sediment supply (e.g., termination of sediment supply and introduction of sediment pulses) in a laboratory flume of forced pool-riffle morphology. We demonstrate that: (1) 1D numerical models can accurately reproduce sediment transport events if applied on a reach-averaged basis; and (2) inadequate consideration of the reach-averaged nature of 1D numerical sediment transport models may result in unrealistic simulation results. In addition, we provide a formulation that allows for a relatively accurate estimate of rates of sand transport as bed load over a gravel-bedded channel by applying a sand transport equation developed for low-land rivers with corrections to bed roughness and partial sand coverage. Ideally, the results presented in the paper

[1]Hydraulic Engineer, Stillwater Sciences, 2855 Telegraph Ave., Ste. 400, Berkeley, CA 94705 (corresponding author). E-mail: yantao@stillwatersci.com

[2]Geomorphologist, Stillwater Sciences, 2855 Telegraph Ave., Ste. 400, Berkeley, CA 94705.

[3]Assistant Professor, Dept. of Geography, Simon Fraser Univ., Burnaby, BC, V5A 1S6, Canada.

[4]Geomorphologist, Stillwater Sciences, 2855 Telegraph Ave., Ste. 400, Berkeley, CA 94705.

[5]Professor, Dept. of Earth and Planetary Science, Univ. of California, Berkeley, CA 94720.

[6]Assistant Professor, Dept. of Geosciences, San Francisco State Univ., San Francisco, CA 94132.

Note. Discussion open until December 1, 2008. Separate discussions must be submitted for individual papers. To extend the closing date by one month, a written request must be filed with the ASCE Managing Editor. The manuscript for this paper was submitted for review and possible publication on December 11, 2006; approved on November 14, 2007. This paper is part of the ***Journal of Hydraulic Engineering***, Vol. 134, No. 7, July 1, 2008. ©ASCE, ISSN 0733-9429/2008/7-892–904/$25.00.

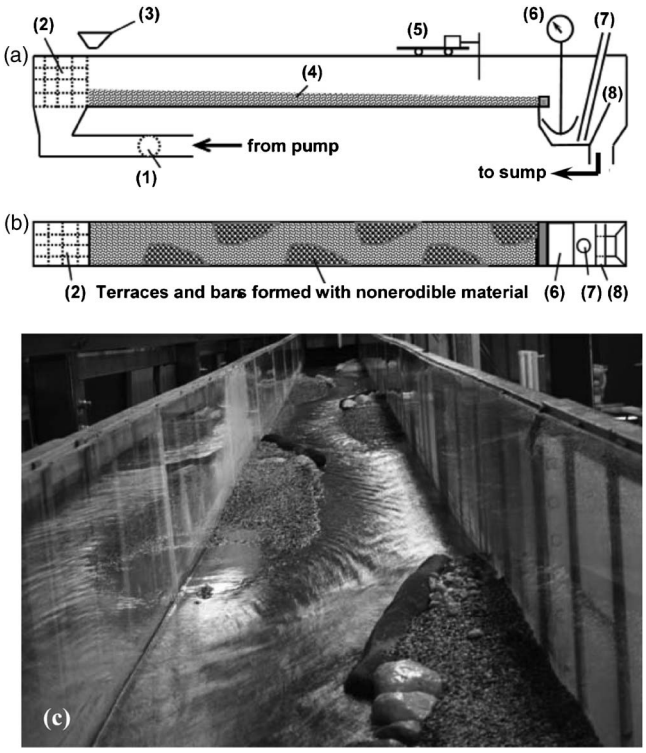

Fig. 1. (a) Sketch of RFS flume and its associated facilities; (b) sketch of plan view of experimental setup; and (c) photograph taken during Run 3 (degradation run), looking upstream. Equipment labeled in the sketches refers to: (1) flow meter; (2) energy dissipater; (3) sediment feeder; (4) sediment deposit; (5) cart and scanners; (6) sediment drum and scale; (7) sediment removal system; and (8) tailgate for water surface regulation. Sketches are not to scale.

will encourage a more widespread adherence to the reach-averaged considerations necessary for 1D numerical sediment transport model applications. Realizing the reach-averaged requirements of 1D models will also provide guidance for how detailed field data should be collected in support of 1D numerical sediment transport modeling. We hope that the good agreement between our 1D numerical simulations and physical model data in a forced pool-riffle morphology will provide the scientific and resource management communities with confidence regarding the performance of 1D numerical sediment transport models if applied on a reach-averaged basis, despite the recently reported poor model performances when 1D numerical sediment transport models were applied in river reaches with pool-riffle morphology (Rathburn and Wohl 2001).

Overview of Flume Experiments

Experiments were conducted in a 28 m long, 0.86 m wide, and 0.6 m deep sediment feed flume at the Richmond Field Station (RFS) of the University of California (Fig. 1). The primary purpose of the experiments was to examine sediment pulses from gravel augmentation or dam removal in a channel with pool-riffle morphology. The flume experiments were designed as generic models of sediment pulse movement and were not scaled to any specific prototype river. Detailed information about the experiments and analyses examining sediment deposition and erosion patterns on a morphologic unit and reach scale as well as comparisons with results from 1D flume experiments will be reported elsewhere. Herein, only a brief experimental overview is provided to introduce information relevant to this paper.

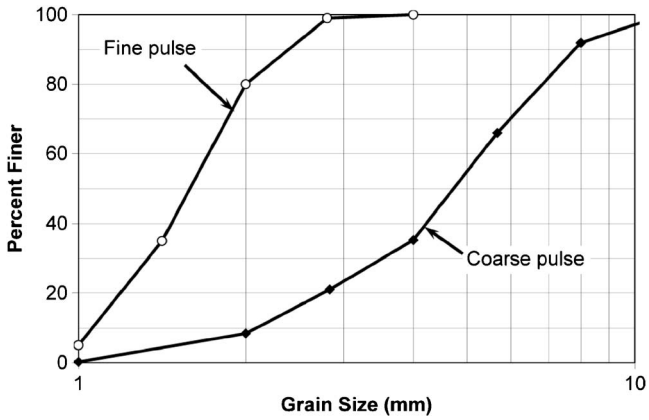

Fig. 2. Grain size distributions for fine and coarse sediment pulses. Sediment used for coarse pulse was also used as sediment feed to establish initial equilibrium bed.

Prior to releasing experimental sediment pulses, the main objective of the initial setup was to create a degraded and armored channel with pool-riffle morphology that would be indicative of conditions downstream of a dam. In order to induce scour and depositional patterns found in natural rivers, sand bags and cobble-sized stones were placed in the flume to force alternating bar sequences [Figs. 1(b and c)]. The sand bags were placed five flume widths apart longitudinally, alternating between the left and right sides of the flume. With the fixed bars in place, constant water discharge (20 l/s) and a constant sediment feed rate (40 kg/hr) were applied until the flume reached an equilibrium state (i.e., the cumulative aggradation and degradation within the flume became minimal and sediment flux at flume exit became almost identical with sediment feed). The water discharge and sediment feed rate were determined through a trial-and-error process so that the resulting reach-averaged channel slope would be close to 0.01, a target predetermined in order to compare these experimental results with previously conducted 1D experiments (i.e., without forced pool-riffle morphology). The sediment used to create the initial equilibrium bed had a geometric mean size of approximately 4.2 mm and a roughly log-normal grain-size distribution (Fig. 2), and was fed from the upstream end of the channel with an automatic sediment feeder [Fig. 1(a)]. Sediment exiting the flume was collected and weighed automatically with an electronic scale logging measurements every 10 s.

Discharge to the flume was periodically shut off in order to measure bed topography, and just prior to shutting off flow, a corresponding water surface profile was surveyed. Bed topography during the experiments was measured with a laser scanner (~1 mm vertical resolution) collecting data every 0.01 m both longitudinally and laterally. Volumetric estimates of the sediment stored in the flume based on topographic scans coupled with sediment feed data were also used to calculate sediment flux at the flume exit based on the principle of mass conservation, which supplemented the sediment flux continuously measured at the flume outlet. Water surface profiles during the experiments were measured with an acoustic scanner (~2 mm vertical resolution) collecting data every 0.06 m longitudinally and every 0.01 m laterally. Topographic scans subtracted from water surface scans

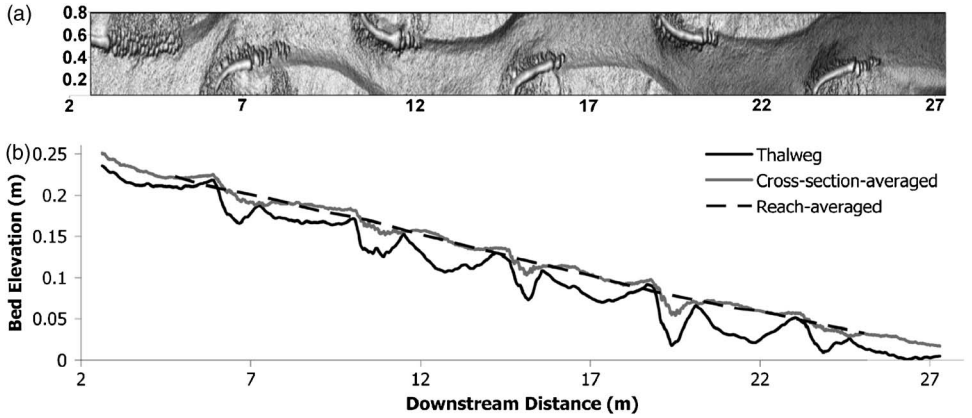

Fig. 3. Equilibrium conditions established under constant 20 l/s water discharge and 40 kg/hr sediment feed: (a) shaded relief map derived from detailed topographic scan; (b) longitudinal bed profile. Flow is from left to right. Three bed profiles are presented in (b): along thalweg (projected onto flume centerline), averaged over wetted cross section width, and reach-averaged profile (moving average over 4.3 m, which is one wave length of forced bar sequences). Bar surfaces (terraces) are excluded in calculating bed profiles presented in (b).

provided detailed water depth grids that were used to calculate average water depths.

The equilibrium morphology associated with 20 l/s water discharge and 40 kg/hr sediment feed had alternating pool and riffle sequences and strong longitudinal topographic variations as indicated by the deep pools along the thalweg (Fig. 3). Riffles formed at the velocity cross-overs at the downstream end of each forced bar sequence. In order to adhere to the reach-averaged nature of 1D numerical sediment transport models, a moving average longitudinal profile was calculated based on measured bed elevations. The reach-averaged bed elevation at every longitudinal station (corresponds to 1 point every 0.01 m) was calculated by averaging all the laser scanned topographic points within the wetted channel area over a 4.3 m long reach (2.15 m upstream and 2.15 m downstream). This corresponds to a moving average over one wavelength of the forced pool-riffle sequence. The resulting reach-averaged initial equilibrium profile had a ~0.0095 slope over the entire flume length with most of the topographic longitudinal variations smoothed out [Fig. 3(b)]. Pool and riffle locations were stationary during the experiments because the sand bags and large pebbles locked them in place and no alternate bar migration occurred. Identical moving averages were calculated for all the measured profiles throughout the experiments to produce reach-averaged profiles for all runs reported in this paper.

After reaching equilibrium under the constant discharge and constant sediment feed, our first experiment (Run 3) modeled conditions downstream of a large reservoir that traps all the upstream bed-load supply. For Run 3 we shut off the sediment feed and continued constant flow at 20 l/s for approximately 66 hr until a second equilibrium profile was achieved (i.e., both channel degradation and sediment flux at the flume exit became minimal). The elimination of sediment supply resulted in significant channel degradation during the run. Degradation was more pronounced at the upstream end of the flume (>0.06 m) and generally decreased in the downstream direction (Fig. 4). Fig. 4 indicates that the reach-averaged change in bed elevation is nearly linear, but there were large, local variations in the thalweg and cross-section-averaged bed elevation changes. The reach-averaged channel slope decreased from ~0.0095 to ~0.0073 by the end of Run 3. Associated with the degradation during Run 3, the surfaces of the forced bars emerged from the flow (at 20 l/s) and functioned as floodplain terraces that did not interact with flow for the remaining experiments [Fig. 1(c)]. Water depth averaged over the entire experimental reach within the wetted area near the end of Run 3 when channel bed reached the new equilibrium was calculated to be 0.087 m.

Six sediment pulse runs (Runs 4, 5, 6, 7, 8, and 10) were conducted following Run 3, each starting with initial conditions similar to the degraded channel bed at the end of Run 3 (Table 1). During each run, either a coarse or a fine sediment pulse was fed manually into the flume at the apex of the upstream-most bar (i.e., approximately 3 m downstream of the channel entrance), representing sediment input due to dam removal, gravel augmentation, landslides, or other short-term sediment input events. The grain-size distribution for the coarse sediment pulse was identical to the original sediment feed used to create the initial equilibrium profile (Fig. 2). The fine sediment pulse had a geometric mean grain size of 1.5 mm and was well sorted as indicated by its low geometric standard deviation of 1.36 (Fig. 2). The sediment pulses were introduced at the beginning of each run at a constant feed rate (different feed rates were used for different runs) for either 1 or 2 hr with flow held constant at 20 l/s (Table 1). Following the termination of the sediment pulse feed, the 20 l/s water discharge continued until the channel bed returned to a similar condition as the post-Run 3 degraded channel and the sediment flux measured at the flume exit became minimal.

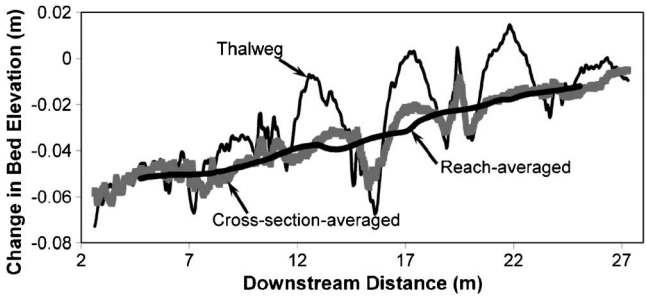

Fig. 4. Change in bed elevation for Run 3 following 66 hr without sediment feed. Bed elevation change is relative to initial equilibrium profiles shown in Fig. 3.

Table 1. Summary of Flume Experiments Investigating Sediment Pulses and Numerical Models Used for Simulations

	Initial reach-averaged slope	Pulse type	Pulse feed rate (kg/hr)	Pulse duration (hr)	Run duration (hr)	Model applied
Run 3[a]	0.0095		Degradation run, no sediment feed		66	DREAM-2
Run 4	0.0073	Coarse	156	1	35	DREAM-2
Run 5	0.0074	Fine	156	1	19	DREAM-1
Run 6	0.0074	Fine	312	2	19	DREAM-1
Run 7	0.0071	Fine	312	2	15	DREAM-1
Run 8	0.0073	Coarse	312	2	56	DREAM-2
Run 10	0.0071	Fine	78	1	9	DREAM-1

[a]Equilibrium run was conducted prior to Run 3, with constant water discharge of 20 l/s and constant coarse sediment feed rate of 40 kg/hr, resulting in equilibrium channel with reach-averaged slope of 0.0095 to start Run 3.

Overview of DREAM-1 and -2

We used the results of the seven flume experimental runs to evaluate the performance of two 1D numerical sediment transport models, DREAM-1 and DREAM-2. The two models are briefly discussed below, and detailed descriptions of the models, including the governing equations, methodology, and sensitivity test to input parameters, can be found in Cui et al. (2006a,b).

DREAM-1 is one of two dam removal express assessment models developed for simulation of sediment transport following dam removal. The model was designed for simulations where the sediment deposit in the reservoir upstream of the dam under consideration for removal is composed primarily of noncohesive fine sediment (i.e., sand and silt). The model simulates the transport and deposition of fine sediment and is applicable to rivers with any combination of sand-bedded, gravel-bedded, and bedrock reaches downstream of the dam. Because the model does not simulate the transport of gravel, it treats gravel beds as immobile so that fine sediment either passes through or deposits within the gravel-bedded reach and potentially transforms it into a sand-bedded reach if the sand deposit becomes thick enough. For flow parameter calculations, the model applies a standard backwater equation (Chaudhry 1993) for low Froude number conditions [i.e., Froude numbers <0.9, see Cui et al. (2006b) for details] and applies a quasi-normal flow assumption [i.e., friction slope is identical to local bed slope; see Cui and Parker (2005)] for high Froude number conditions. The model applies the Brownlie (1982) bed material equation for calculating sediment transport capacity and considers the entire range of fine sediment (sand and silt) as one unit for mass conservation calculations. The model requires the following input parameters: Initial channel profile, initial thickness of fine sediment deposits in the reservoir and downstream reaches, channel cross sections simplified as rectangles with widths equal to the bankfull channel width, water discharge, the rate and size of sediment supply, and the downstream base-level control (i.e., either downstream water surface elevation or fixed bed elevation). Model output includes the evolution of the thickness of fine sediment deposits in the upstream reservoir and in downstream reaches and sediment flux along the river in response to the specified water discharge and sediment supply conditions.

For DREAM-1 simulations of sand transport over a gravel-bedded channel presented in this paper, a simple roughness correction and a partial sand coverage correction are introduced to adjust the sand transport rate calculated with the Brownlie (1982) bed material equation (Fig. 5). The corrections are presented in more detail with derivations in the Appendix. A roughness correction is needed because the Brownlie (1982) formulation calculates bed roughness (denoted as k_s hereafter) based entirely on sand particle size in transport, since the equation was developed for application in sand-bedded rivers. However, for sand transport over a gravel bed, the bed is rougher than a sand-bedded channel at the grain size scale if the gravel bed is not completely covered with sand. Under these conditions, the stress exerted on the gravel particles will not be available for transport of fine sediment. Thus, a correction is introduced to adjust the overall roughness and partitioning the shear stress into that exerted on roughness elements (gravel particles in this case, and assumed to be immobile) and that exerted for sediment transport. No roughness adjustments are made due to the pool-riffle morphology for the following reasons: (1) Sand-bedded rivers also have similar features such as pools associated with channel curvatures and alternate bars, and, thus, their influence on sediment transport should already be at least partially included in the original sediment transport equation; (2) while the added friction from the pool-riffle features may act to reduce sediment transport efficiency, the increased complexity in channel cross sections due to pool-riffle morphology may act to increase the efficiency for sediment transport due to the nonlinear relation between sediment transport and shear stress, and it is not clear what is the combined effect from the combination of the two.

A partial sand coverage correction is needed in instances where the sand covers only a portion of the channel because sand

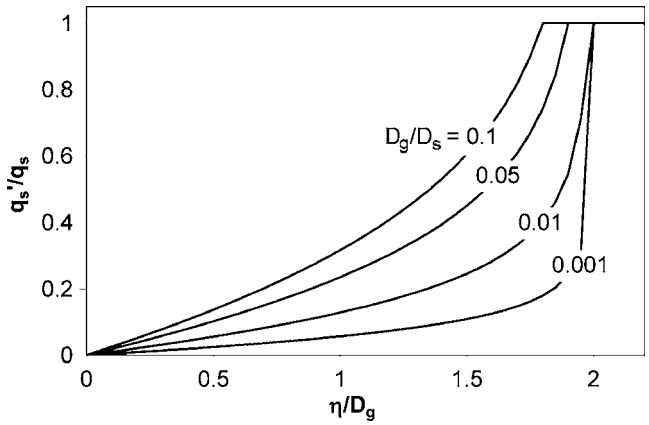

Fig. 5. Corrections to calculated sand transport capacity for sand transport over gravel bed, in which q_s=sand transport rate calculated with sand transport equation; q_s'=sand transport rate with roughness and partial area coverage corrections; η=thickness of sand deposit over gravel bed; D_g=geometric mean grain size of gravel bed material; and D_s=geometric mean of sand particles in transport

transport equations always assume that sand covers the entire bed.

The corrections described in the Appendix affect sand transport only when the sand deposit is extremely thin (i.e., not thick enough to cover the gravel bed), as shown in Fig. 5. The introduced corrections result in improved simulation results for small sand pulse runs and improved sand flux predictions during a short period of time following the introduction of sand pulses when the sand barely covers the gravel bed. This adjustment has minimal effects on bed aggradation and degradation for large sand pulses.

DREAM-2 is the second model developed for simulation of sediment transport following dam removal. The model is designed for simulations where the sediment deposit in the reservoir upstream of the dam under consideration for removal is either composed primarily of coarse sediment (i.e., gravel and coarser) or is stratified with the top layer composed primarily of coarse sediment. The model simulates the transport and deposition of both coarse and fine sediment and can be used in rivers with a combination of gravel-bedded and bedrock reaches. DREAM-2 uses the same methods as DREAM-1 for calculating flow parameters. For sediment transport, DREAM-2 applies the Brownlie (1982) bed material equation for calculating fine sediment transport capacity and the Parker (1990) bed-load equation for calculating coarse sediment transport capacity. For sediment continuity, DREAM-2 considers the mass conservation of sediment in different size groups, and includes the abrasion of coarse sediment during its transport downstream that gradually reduces the size of coarse particles and produces silt and a small fraction of sand. The model requires the following input parameters: Initial channel profile, initial thicknesses of fine and coarse sediment deposits in the reservoir and downstream reaches, initial surface and subsurface grain-size distributions along the river, channel cross sections simplified as rectangles with widths equal to the bankfull channel width, water discharge, the rate and grain-size distribution of sediment supply, volumetric abrasion coefficients for coarse sediment (i.e., fraction of particle volume lost per unit distance traveled, assumed to be zero for simulations conducted in this paper because of the short distance traveled by sediment particles), and downstream base-level control. Model output includes the evolution of the thicknesses of fine and coarse sediment deposits, sediment flux rates and grain-size distributions, and the grain-size distributions of surface and subsurface sediment along the river in response to the specified water discharge and sediment supply conditions.

The surface-based bed-load equation of Parker (1990) used in DREAM-2 was developed based on field data, and its application to flume conditions often requires a simple adjustment to the reference Shields stress [e.g., (Cui et al. 1996, 2003); see Parker (1990) for definition of reference Shields stress]. For simulations presented in this paper, reference Shields stress was adjusted from its original value of 0.0386 to 0.0444 so that the sediment transport model produced the observed reach-averaged slope of 0.0095 at 20 l/s water discharge and 40 kg/hr sediment feed during the initial equilibrium run. Other than this reference Shields stress adjustment, no further calibrations were made for simulating the coarse sediment runs with DREAM-2.

As mentioned above, both DREAM-1 and DREAM-2 simplify channel cross sections as rectangular channels with widths that are equal to bankfull channel widths and bottom elevations that are equal to the reach-averaged bed elevation. In the simulation presented below, the bankfull channel width was assumed to be half of the flume width (0.43 m) based on observations of the average wetted channel width during the flume experiments.

Comparison of DREAM-1 and DREAM-2 Simulations with Flume Results

Numerical simulations were conducted for seven runs with either DREAM-1 or DREAM-2 based on model suitability for fine or coarse sediment pulses, as listed in Table 1. The initial reach-averaged slope used as input for the numerical simulations was calculated based on the reach-averaged profile of the experimental data for each run and was almost identical to the reach-averaged slope at the end of Run 3 (Table 1). Herein, detailed results from two numerical runs are presented: Run 7 for DREAM-1 simulation and Run 8 for DREAM-2 simulation. The two runs were chosen because Runs 7 and 8 were the two largest (i.e., highest feed rate and volume) fine and coarse sediment pulse experiments, respectively (note: Run 6 was a replica of Run 7 with very similar results).

Comparison between simulated results and flume measurements for Run 7 are presented in Figs. 6–8 and for Run 8 in Figs. 9–11. Figs. 6 and 9 illustrate the evolution of the reach-averaged longitudinal profiles, Figs. 7 and 10 show the changes in reach-averaged bed elevation relative to the initial bed, and Figs. 8 and 11 display the sediment flux and cumulative sediment transport at the flume exit. Results depicted in Figs. 6, 7, 9, and 10 demonstrate that both DREAM-1 and -2 closely reproduced the aggradational and degradational patterns associated with the introduction of fine and coarse sediment pulses.

Comparing simulated and measured sediment flux and cumulative sediment transport for Run 7 (Fig. 8) indicates that DREAM-1 reproduced the measured sediment transport data well, including the general pattern and magnitude of the sediment flux time series and the magnitude of cumulative sediment transport at the flume exit. The simulated cumulative sediment transport at the end of the run is only 3.6% higher than the flux measured at the flume outlet and 10% lower than a flux estimate based on mass conservation calculated with sediment pulse input and laser scanned topography.

A similar comparison of simulated and measured sediment flux and cumulative sediment transport at flume exit for Run 8 (Fig. 11) indicates that DREAM-2 reproduced the general patterns of the sediment flux time series, but does not achieve the same level of precision in matching the flume data as the DREAM-1 simulation. In particular, the simulated sediment flux at the flume exit is advancing ahead of experimental curve by approximately 1 hr [Fig. 11(a)]. The comparison in Fig. 11(b) indicates that the simulated magnitude of sediment transport was generally within a factor of 2 of the measured data. At the end of the run, the simulated cumulative transport at the flume exit is 70% higher than the flux measured at the flume outlet and 34% higher than a flux estimate based on mass conservation calculated with sediment pulse input and laser scanned topography. The difference between simulated and measured cumulative sediment transport at the flume exit can in part be attributed to some of the sediment pulse depositing and stabilizing on the lateral margins of the bars and not transporting out of the flume during the experiment. In 1D numerical model simulation, however, the simulated bed profile always returns to its initial equilibrium state if constant discharge is maintained and the sediment feed is terminated. Comparatively, for Run 7 nearly 100% of the fine sediment pulse exited the flume and, thus, the better agreement between measured and modeled cumulative sediment flux for that run. Accuracy in predicted sediment transport rates within a factor of 2 is usually considered in good agreement for sediment transport modeling, which is evident in most comparisons between simu-

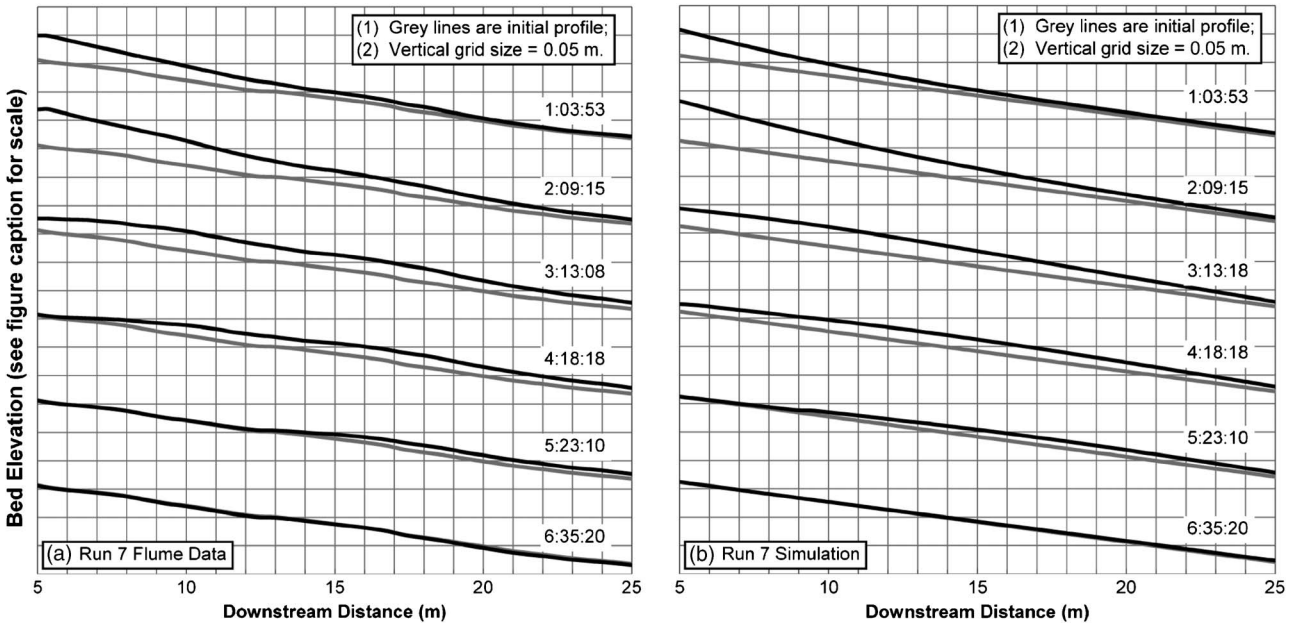

Fig. 6. Comparison of measured and simulated reach-averaged bed profiles for Run 7 (large fine sediment pulse run): (a) flume measurement; (b) DREAM-1 simulation. Time steps in diagrams reference time relative to start of sediment pulse feed, in hour:minute:second.

lated and calculated sediment transport rates where results are plotted in a log scale due to the large scatter of the measured data (Gomez and Church 1989; Brownlie 1982). Sediment transport predictions within a factor of 2 appear acceptable for our experiments as illustrated by the good agreement between simulated and measured changes in reach-averaged bed elevations shown in Figs. 9 and 10.

The performance of the two models was also examined quantitatively, using the comparisons of predicted and measured change in reach-averaged bed elevation. For each run, we compared the simulated change in bed elevation (i.e., the amount of aggradation or degradation from the start of the run, denoted as $\Delta\eta_s$) with measured change in reach-averaged bed elevation (denoted as $\Delta\eta_m$) and calculated the error associated with the

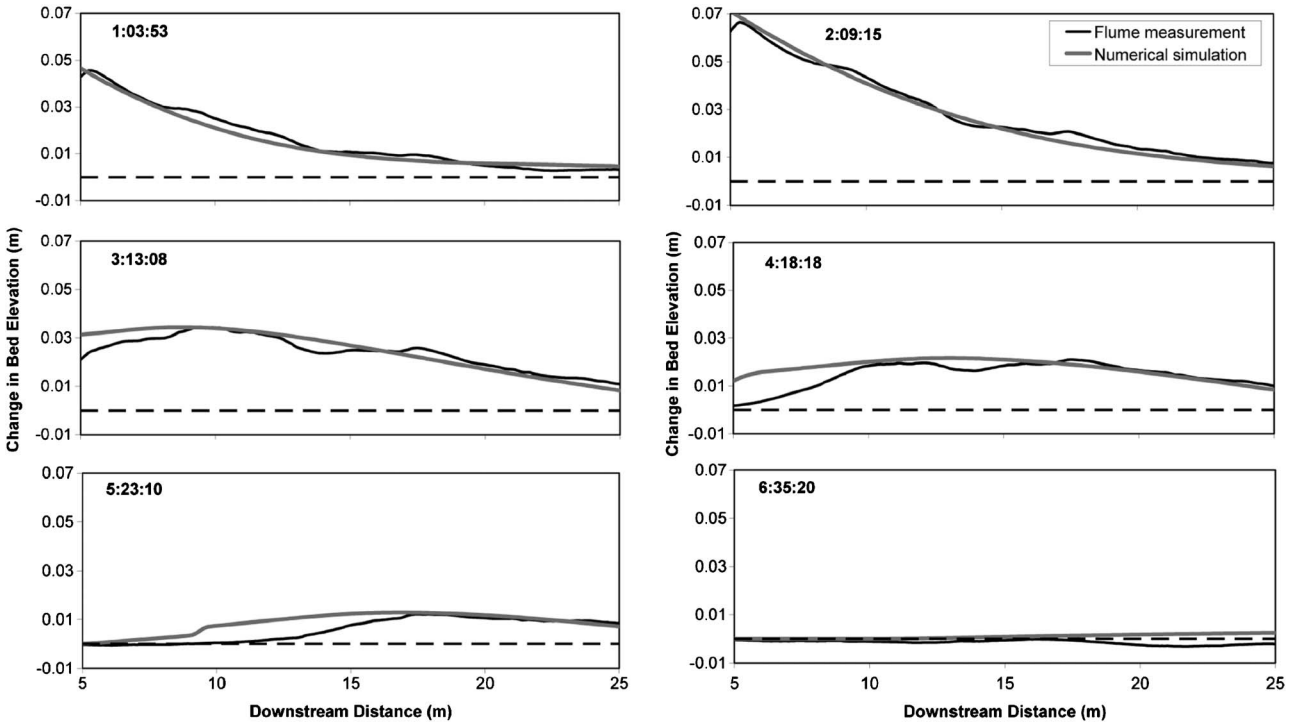

Fig. 7. Comparison of measured and simulated change in reach-averaged bed elevation relative to initial reach-averaged bed for Run 7 (large fine sediment pulse run). Time steps in diagrams reference time relative to start of sediment pulse feed, in hour:minute:second.

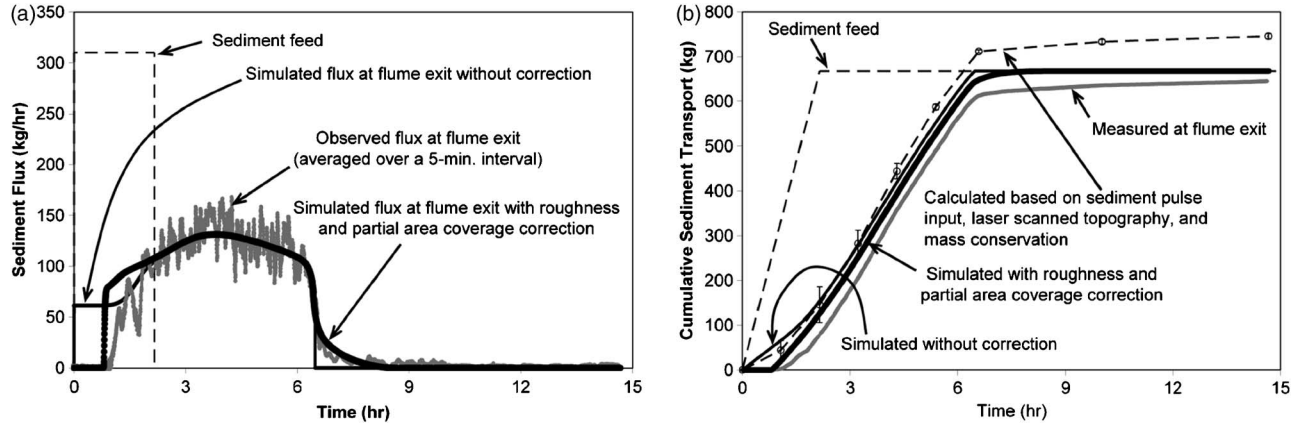

Fig. 8. Measured and simulated sediment transport at flume exit for Run 7: (a) Sediment flux; (b) cumulative sediment transport. Cumulative transport calculated based on mass balance of sediment pulse input and laser scanned topography assumes density of 2,650 kg/m^3 for sediment particles and porosity of 0.35. Error bars denote potential range if calculation assumes a porosity of 0.3 and 0.4. Simulated results without sand transport rate corrections for roughness and partial area coverage are also presented.

numerical simulation as $\varepsilon=|\Delta\eta_s-\Delta\eta_m|$ between 5 and 25 m downstream of the flume entrance with a 1-*m* spacing (i.e., a total of 21 points equally spaced between 5 and 25 m). The ε values at the 21 locations at the time intervals with measured topography were then used collectively for statistical analysis to derive a model performance curve, as shown in Fig. 12. The model performance curve has the error in simulated change in reach-averaged bed elevation on the *x*-axis and the corresponding percent of samples with errors smaller than this value (nonexceedance probability) on the *y*-axis. For example, the performance curve for Run 7 (Fig. 12) has a coordinate of 3 mm and 70%, which indicates that 70% of the samples have errors smaller than 3 mm for this run.

DREAM-1 model performance curves for Runs 5, 7, 10, and a comprehensive performance curve combining all the DREAM-1 simulations are presented in Fig. 12. Based on the comprehensive curve, the largest error for any DREAM-1 simulation is approximately 12.2 mm, 84% of the samples have errors less than 3.3 mm, 50% of the samples have errors less than 1.5 mm, and 16% of the samples have errors less than 0.6 mm. Similar perfor-

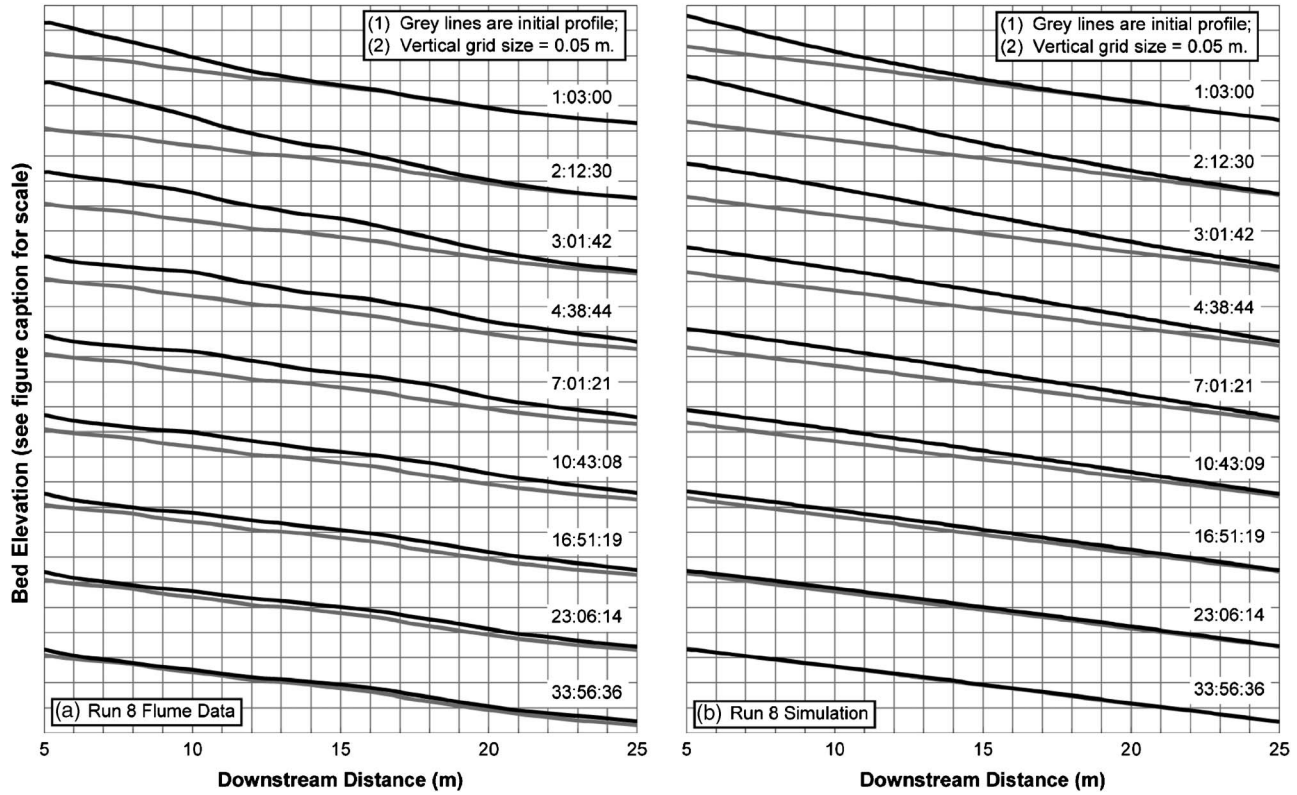

Fig. 9. Comparison of measured and simulated reach-averaged bed profiles for Run 8 (large coarse pulse run): (a) flume measurement; (b) DREAM-2 simulation. Time steps in diagrams reference time relative to start of sediment pulse feed, in hour:minute:second.

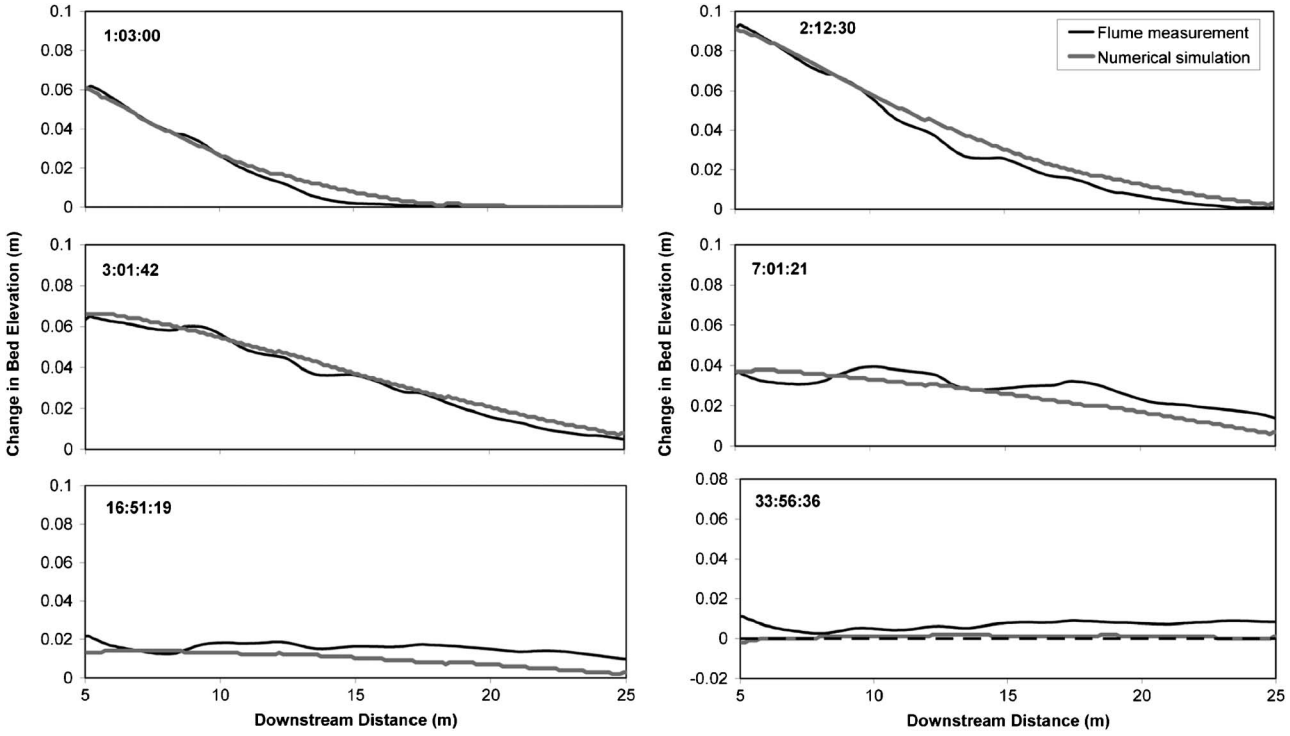

Fig. 10. Comparison of measured and simulated change in reach-averaged bed elevation relative to initial reach-averaged bed for Run 8 (large coarse pulse run). Time steps in diagrams reference time relative to start of sediment pulse feed, in hour:minute:second.

mance curves for DREAM-2 simulations are presented in Fig. 13, including a combined performance curve based on Runs 3, 4, and 8, indicating that the largest error in simulated reach-averaged change in bed elevation is approximately 14.2 mm, 84% of the samples have errors less than 7.0 mm, 50% of the samples have errors less than 3.9 mm, and 16% of the samples have errors less than 1.0 mm.

A summary of performance measures are presented in Table 2, showing the simulation errors relative to the geometric mean grain size of the coarse pulse (D_g) of 4.2 mm, relative to the average water depth measured near the end of Run 3 (0.087 m, denoted as $\bar{H}$ hereafter), and their absolute values. The average water depth at the end of Run 3 is chosen to scale the simulation errors because the bed profile at the end of Run 3 is almost identical to the initial bed profile of all the subsequent runs. We reiterate that the coarse pulse sediment was also used to create the initial channel bed for all the runs, so it can be viewed as a surrogate for the bed material size distribution in the absence of bed material samplings. Relative to the geometric mean grain size of the coarse sediment, 84% of the samples have simulation errors within $0.77D_g$ for DREAM-1 simulations, and 84% of the samples have simulation errors within $1.65D_g$ for DREAM-2 simulations. Relative to average water depth, 84% of the samples have simulation errors less than $0.037\bar{H}$ for DREAM-1 simulations, and 84% of the samples have simulation errors less than

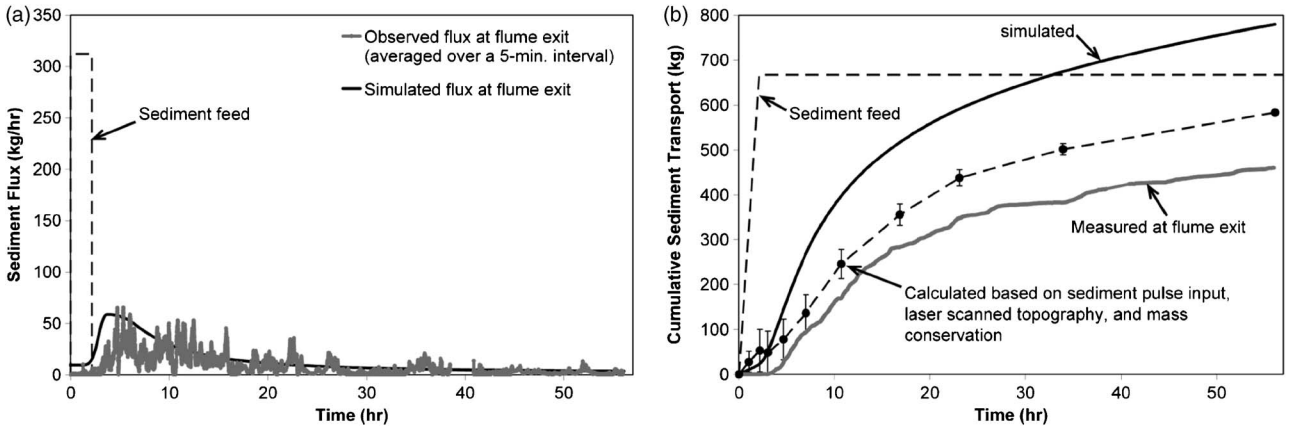

Fig. 11. Measured and simulated sediment transport at flume exit for Run 8 (large coarse pulse run): (a) sediment flux; (b) cumulative sediment transport. Cumulative transport calculated based on sediment pulse input and laser scanned topography assumes density of 2,650 kg/m^3 for sediment particles and sediment deposit porosity of 0.35. Error bars denote the potential range if the calculation assumes porosity of 0.3 and 0.4.

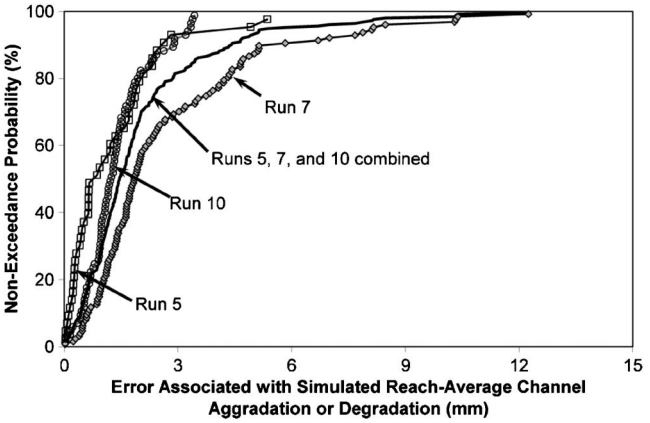

Fig. 12. Performance curves for DREAM-1, based on simulations of fine sediment pulse Runs 5, 7, and 10

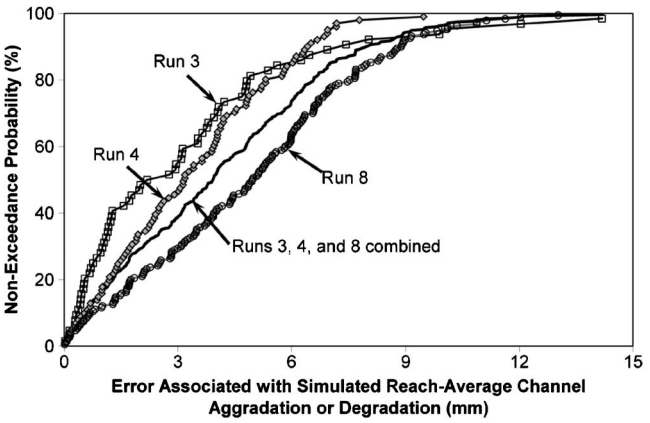

Fig. 13. Performance curves for DREAM-2, based on simulations of coarse sediment degradation run (Run 3) and coarse sediment pulse runs (Runs 4 and 8)

$0.11\bar{H}$ for DREAM-2 simulations. Figs. 12 and 13 and Table 2 illustrate that Runs 7 and 8 have the largest errors in simulated reach-averaged bed aggradation or degradation for the runs simulated with DREAM-1 and -2, respectively. Runs 7 and 8 are also the model simulations presented in detail earlier and similar plots for simulations of other pulses typically show similar or better agreements than those presented here (Figs. 6, 7, 9, and 10).

As discussed earlier, the flume experiments were conducted to examine the evolution of sediment pulses for a generic river system with pool-riffle morphology and were not scaled to a specific prototype river. For evaluating potential model performance in natural rivers, we expect that modeling errors relative to bed material geometric mean grain size or relative to water depth would be somewhat higher than observed for flume simulations because of the added complexity in natural rivers.

Discussions

It is important to realize that the reach-averaged principle for 1D numerical sediment transport simulation does not suggest that detailed topographic data in the field need to be collected in order to obtain reach-averaged bed profiles, even though detailed topographic data collection in the field is becoming increasingly feasible with the availability of the water penetrating Green LiDAR technology (Jim McKean, personal communication, December 2006). On the contrary, it suggests that initial bed profile for 1D numerical sediment transport model simulation should be less detailed so that topographic features incompatible with the reach-averaged nature (e.g., detailed pool-riffle topography) is ignored in the simulation. Under large spatial scale situations, 1D numerical sediment transport models usually have to be applied at a rather low spatial resolution, typically with spatial increment (i.e., spacing for longitudinal discretization) on the order of several channel widths or larger. Using a low spatial resolution longitudinal profile will typically "smooth out" local topographic features, but additional steps may still be needed to further average the longitudinal profile. For example, Cui and Wilcox (2008) and Cui et al. (2006a,b) apply a "zeroing-process" to generate an initial longitudinal profile for 1D model simulations, and HEC-6 simulations often need the initial longitudinal profile to be

Table 2. Summary of Errors in Simulated Reach-Averaged Aggradation/Degradation Compared to Measured Flume Results[a]

Nonexceedance probability	16%			50%			84%		
Variable	ε (mm)	ε/D_g	$\varepsilon/\bar{H}$	ε (mm)	ε/D_g	$\varepsilon/\bar{H}$	ε (mm)	ε/D_g	$\varepsilon/\bar{H}$
DREAM-1									
Run 5	0.2	0.05	0.0026	0.8	0.18	0.0087	2.3	0.55	0.027
Run 7	0.9	0.22	0.011	1.8	0.44	0.021	4.7	1.11	0.053
Run 10	0.6	0.14	0.0067	1.2	0.29	0.014	2.3	0.54	0.026
Runs 5, 7[b], and 10 combined	0.6	0.14	0.0069	1.5	0.35	0.017	3.3	0.77	0.037
DREAM-2									
Run 3	0.5	0.11	0.0054	2.2	0.52	0.025	5.6	1.32	0.064
Run 4	1.0	0.24	0.011	3.2	0.75	0.036	5.9	1.40	0.067
Run 8	1.6	0.37	0.018	5.0	1.18	0.057	7.9	1.88	0.091
Runs 3, 4, and 8 combined	1.0	0.24	0.011	3.9	0.94	0.045	7.0	1.65	0.11

[a]D_g=4.2 mm denotes geometric mean grain size of gravel pulse (Fig. 2); and $\bar{H}$=0.087 m denotes average water depth at beginning of run.
[b]Data from Run 6 are not analyzed because they are replicate of Run 7 with very similar results.

"primed" (ACOE 1993; Bountry and Randle 2001). In these cases, a 1D numerical model was run for a significant period of time with the measured longitudinal profile as an initial condition in conjunction with recorded hydrologic data and best estimates of sediment supply as inputs. This simulation produces a longitudinal profile that is similar to the measured initial condition bed profile, but smoothes out some of the topographic features that cannot be reproduced with a 1D numerical sediment transport model (i.e., some of the pools that aggraded and some of the bars that degraded during the simulation). This simulated longitudinal profile, which can be viewed as a representation of the reach-averaged profile of the river, was than used as the initial condition for ensuing sediment transport simulations so that any subsequent sediment deposition and erosion can be viewed as the direct result due to changes in sediment supply or hydrologic conditions (the intended objective of the simulations). In the numerical simulations of the experimental runs presented in this paper, our initial profile for Run 3 (the first run) was set as a planar bed with a slope of 0.0095. This initial condition is similar to the longitudinal profile that would be produced through a "zeroing process" by running the model for an extended period of time, starting with the measured longitudinal profile along the thalweg and supplying the flume with a 20 l/s water discharge and a 40 kg/hr sediment feed. Thus, our simulations presented in this paper are consistent with the "zeroing process" or "priming" the initial longitudinal profile practices discussed above.

The zeroing process or model prime should produce a longitudinal profile similar to the existing channel longitudinal profile void of some localized topography. If either process produces a longitudinal profile that deviates significantly from the current profile, it indicates either the input parameters (hydrology or sediment supply) are not accurate or that the model itself needs calibration. Consequently, the zeroing process or model prime can also be viewed as model validation or at least a part of a model calibration process. For example, in the simulations presented in this paper, our initial simulations produced a channel with a slope that significantly deviated from the measured average bed slope of 0.0095 at 20 l/s discharge and 40 kg/hr sediment supply when using a reference Shields stress of 0.0386 as provided in the original sediment transport equation. We then calibrated the model by modifying the reference Shields stress to 0.0444, which produced the measured average bed slope of 0.0095.

It is important for practitioners to resist the temptation of using overly detailed topographic data for 1D model input and producing results with excessive resolution (i.e., at a pool-riffle scale) simply because such input data are more readily available due to advancements in survey technology. Details in excess of what is compatible with the reach-averaged nature of 1D numerical sediment transport models will likely not improve the quality of modeling results. To demonstrate this, Runs 7 and 8 are simulated with DREAM-1 and -2, respectively, by adding more detailed bed profiles to the simulations. Instead of using the reach-averaged profiles (i.e., an initial profile with a constant slope) for the simulations reported earlier in this paper, the new simulations use the measured thalweg profile as the initial profile. The simulated results are reported as changes in bed elevation and compared with the measured data (Figs. 14 and 15 for Runs 7 and 8, respectively). Comparing Figs. 14 and 15 with Figs. 7 and 10, respectively, the results reported in Figs. 14 and 15 are less accurate than the results for the reach-averaged simulations and are inadequate reproductions of the measured sediment aggradation and degradation patterns. For the new simulations that applied the detailed thalweg profile as the initial profile, model errors are

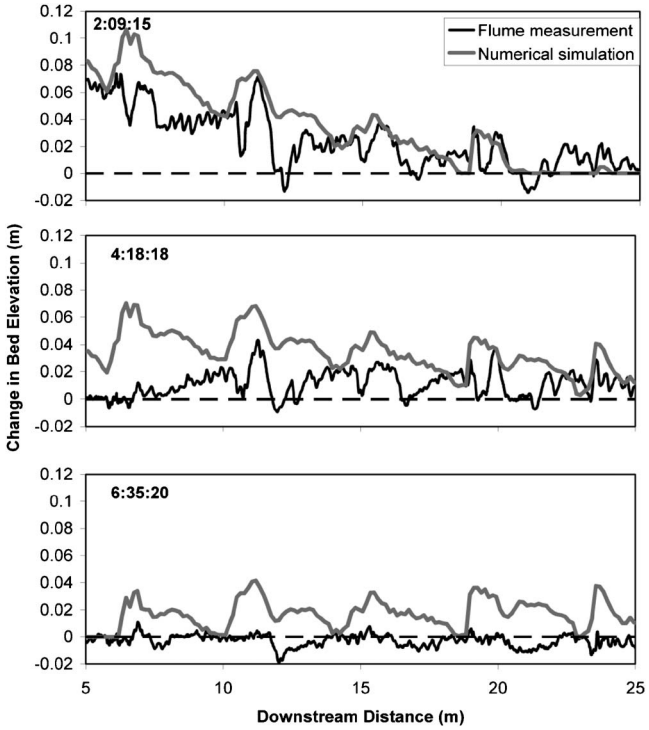

Fig. 14. Comparison of measured and simulated change in bed elevation for Run 7 (large fine sediment pulse run) without reach averaging, demonstrating decreased model performance following mishandling of initial condition in comparison with the reach-averaged results presented in Fig. 7. Numerical simulation used the thalweg elevation as model input, and measured change in bed elevation is calculated based on the surveyed thalweg elevation data. Time steps in diagrams reference time relative to start of sediment pulse feed, in hour:minute:second.

calculated relative to the measured changes in bed elevation along the thalweg of the flume channel, and are then compared with the errors for the reach-averaged simulations in Table 3. Results in Table 3 further illustrate the greater error when using the thalweg as an initial profile.

The two 1D numerical transport models examined in this paper approximate channel cross sections with rectangles that completely neglect the existence of floodplains. This is an important assumption that necessitates further exploration. Two reasons make this simplification work for the majority of modeling applications: (1) overbank flow events usually occur only for a small fraction of time, and, thus, the cumulative sediment transport during those events usually accounts for only a small part of the overall sediment transport despite the fact that overbank flow events are always associated with significant sediment transport (Goodwin 2004); and (2) potential simulation errors introduced by neglecting the existence of floodplains during overbank flow events are usually collectively accounted for with the many other modeling uncertainties (e.g., in hydrology and sediment supply) in the calibration process that includes a period of time with different flow events, including overbank flow events. Thus, approximating cross section geometry with rectangles will normally produce satisfactory results at the reach-averaged scale in natural rivers for most applications.

The corrections applied to calculations of sand transport capacity over a gravel bed improved the quality of DREAM-1 simulations, particularly when the introduced sand pulse was small

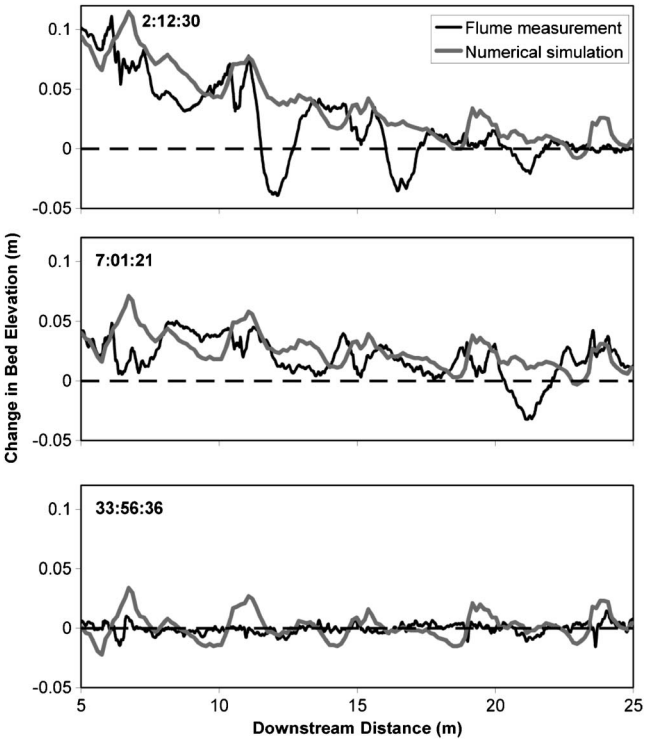

Fig. 15. Comparison of measured and simulated change in bed elevation for Run 8 (large coarse pulse run) without reach averaging, demonstrating decreased model performance following mishandling of initial condition in comparison with reach-averaged results presented in Fig. 10. Numerical simulation used thalweg elevation as model input, and measured change in bed elevation is calculated based on surveyed thalweg elevation data. Time steps in diagrams reference time relative to start of sediment pulse feed, in hour:minute:second.

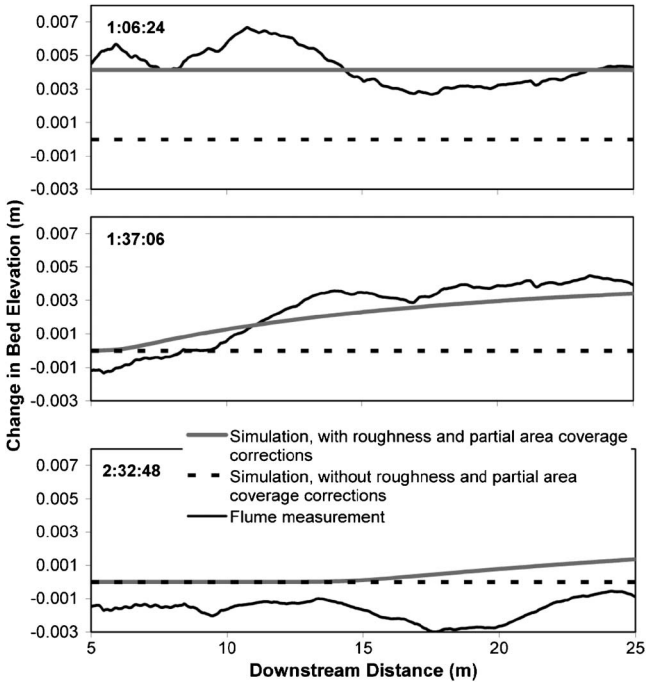

Fig. 16. Simulated (with and without roughness and partial area coverage corrections) and measured changes in reach-averaged bed elevation for Run 10 (run with smallest fine sediment pulse). Important observations include: (1) DREAM-1 simulation without roughness and partial area coverage corrections produced no change in bed elevation during run, while simulated changes in bed elevation with proposed corrections have same pattern as observations, and are within 2 mm ($\sim 0.5D_g$) of measured values except at end of run; and (2) DREAM-1 simulations did not reproduce degradation at end of run because initial gravel bed was assumed to be immobile within the model. Time steps in diagrams reference time relative to start of sediment pulse feed, in hour:minute:second.

(Runs 5 and 10). A comparison of simulated change in bed elevation with and without the proposed corrections for Run 10 (the run with the smallest fine sediment pulse volume) is presented in Fig. 16 with the measured flume data. Fig. 16 demonstrates that the simulated reach-averaged bed aggradation or degradation with the proposed corrections has the same pattern as observed in the flume, and is within 2 mm ($\sim 0.5D_g$) of the measurement, whereas no change in bed elevation was produced for the simulation without the proposed corrections. For larger sand pulses, the improvement is primarily at the onset of sand pulse introduction and after most of the sand pulse exited the flume [Fig. 8(a)], because at these times the sand deposit was not thick enough to cover most of the gravel bed. For large sand pulse runs, the enhanced prediction in sand flux yielded a limited improvement in predicted cumulative sand transport [Fig. 8(b)], and an even smaller improvement in predicted change in bed elevation. Other than the improvement to the simulated changes in bed elevation

Table 3. Comparison of Errors in Simulated Aggradation/Degradation from Two Methods: (1) Using Reach-Averaged Initial Profile and (2) Using Detailed Thalweg as Initial Profile and Ignoring Reach-Averaged Nature of 1D Modeling[a,b]

Nonexceedance probability	16%			50%			84%		
Variable	ε (mm)	ε/D_g	$\varepsilon/\bar{H}$	ε (mm)	ε/D_g	$\varepsilon/\bar{H}$	ε (mm)	ε/D_g	$\varepsilon/\bar{H}$
DREAM-1									
Run 7, reach-averaged simulation	0.9	0.22	0.011	1.8	0.44	0.021	4.7	1.11	0.053
Run 7, using thalweg as initial profile	2.8	0.66	0.032	15	3.54	0.17	33	7.78	0.38
DREAM-2									
Run 8, reach-averaged simulation	1.6	0.37	0.018	5.0	1.18	0.057	7.9	1.88	0.091
Run 8, using thalweg as initial profile	3.3	0.77	0.037	9.2	2.18	0.11	24	5.68	0.27

[a]D_g=4.2 mm denotes geometric mean grain size of gravel pulse (Fig. 2); and $\bar{H}$=0.087 m denotes average water depth at beginning of run.

[b]In calculating ε values for simulations using thalweg as initial profiles, measured changes in bed elevation were calculated based on surveyed thalweg elevations.

and sediment flux when sand is not thick enough to cover the gravel bed, the proposed corrections provide a way to estimate sand transport rates in gravel-bedded rivers by applying sand transport equations developed for low land rivers in situations where the gravel particles on the channel bed are mostly immobile.

Conclusions

Seven flume experiments modeling fine and coarse sediment pulses in forced pool-riffle morphology were successfully simulated with two 1D numerical sediment transport models, DREAM-1 and DREAM-2. Based on simple physical relations, corrections for roughness and partial sand coverage were introduced to DREAM-1 for calculating sand transport capacity when the predicted sand thickness over the gravel bed is insufficient to cover the gravel particles. DREAM-1 is then applied to simulate the fine sediment pulse experiments without further calibration. The only calibration applied to DREAM-2 was adjusting the reference Shields stress in Parker (1990) from its original value of 0.0386 to 0.0444 so that the model produced an equilibrium bed slope identical to the observed reach-averaged slope (0.0095) under a constant discharge (20 l/s) and a constant sediment feed (40 kg/hr).

Comparisons between numerical simulations and experimental data indicate that on a reach-averaged basis, both DREAM-1 and -2 accurately reproduce the bed aggradation and degradation patterns and to a slightly lesser extent the sediment flux at the flume exit. DREAM-1 reproduced the sediment flux at the flume exit for fine sediment pulses better than DREAM-2 did for coarse pulses. Based on comparisons between numerical simulations and flume measurements for changes in reach-averaged bed elevation, 84% of the DREAM-1 results have errors less than 3.3 mm, which is less than 1 geometric mean grain size of the bed material, or approximately 3.7% of the average water depth. In a similar comparison, 84% of the DREAM-2 results have errors less than 6.9 mm, which is less than 2 geometric mean grain sizes of the bed material, or approximately 11% of the average water depth. Simulation results from the same two models with topographic input data more detailed than a reach-averaged longitudinal profile produced results with much higher errors than reach-averaged simulations and unrealistic aggradational and degradational patterns. This supports our recommendation that 1D sediment transport numerical models should only be applied on a reach-averaged basis.

Acknowledgments

Funding for this study was provided by CALFED Ecosystem Restoration Program (Grant No. ERP-02D-P55). The writers appreciate the guidance from the project's scientific advisory committee members: Thomas Lisle, Scott McBain, Gary Parker, Kris Vyverberg, and Peter Wilcock, and the strong support from former and current Stillwater project directors: Frank Ligon, Craig Fixler, and Pete Downs. This manuscript benefited greatly from the very constructive comments to previous drafts by Derek Booth, Frank Ligon, two anonymous reviewers, and the associate editor.

Appendix. Simple Corrections to Predicted Sand Transport as Bed Load over Gravel Bed due to Gravel Particle Roughness and Partial Sand Coverage

Sediment transport equations are generally developed under the assumption that the underlying channel bed is composed of sediment particles resulting from the deposition of sediment particles in transport. The conditions simulated by DREAM-1, however, include the transport of sand particles over a gravel bed, which differs from the conditions under which the Brownlie (1982) sediment transport equation was developed. Two corrections are needed to adjust the sand transport capacity calculated with a sediment transport equation originally designed expressly for sand transport: (1) A correction for the roughness difference between a gravel bed and a sand bed at the grain size scale, and a partition of the energy exerted on sand particles and gravel particles, and (2) a correction for partial coverage of the channel bed with sand. Here we describe the two simple corrections applied in DREAM-1 simulations presented in this paper. The corrections, combined with a sand transport equation, can be used elsewhere for an estimate of the sand transport rate in gravel bedded rivers during low and intermediate flow events when the gravel particles on channel bed are immobile.

Correction to Roughness Formulation

Considering a thin layer of sand transporting over a gravel bed, where the sand layer is not thick enough to cover the entire gravel bed, a Manning-Strickler equation can be used to describe the overall resistance

$$\frac{q_w/h}{\sqrt{\tau_o/\rho}} = 8.1\left(\frac{h}{k_o}\right)^{1/6} \tag{1a}$$

$$\frac{q_w/h_s}{\sqrt{\tau_s'/\rho}} = 8.1\left(\frac{h_s}{k_s}\right)^{1/6} \tag{1b}$$

in which q_w=water discharge per unit width; h=water depth; τ_o=overall shear stress; ρ=density of water; k_o=overall roughness height of the gravel-bedded channel covered with some sand; h_s and τ_s'=water depth and shear stress calculated in DREAM-1, in which roughness height k_s that is proportional to sand diameter is used for the calculation instead of using the overall roughness height k_o.

Manipulating Eqs. (1*a*) and (1*b*), the following expression is obtained:

$$\frac{\tau_s'}{\tau_s} = \left(\frac{k_s}{k_0}\right)^{7/30} \tag{2}$$

It can be expected that the Shields stress for sand particles in a gravel-bedded channel is usually relatively high, and, thus, sand transport equations can usually be approximated as (Meyer-Peter and Müller 1948)

$$q_s \propto \tau_s^{3/2} \tag{3}$$

in which q_s=sand transport capacity per unit width calculated with a sand transport equation. Between Eqs. (2) and (3), sand transport capacity calculated with sand transport equations can be approximately corrected as

$$q_{sr} = \left(\frac{k_s}{k_o}\right)^{7/20} q_s \tag{4}$$

in which q_{sr}=corrected sand transport capacity per unit width for sand transport over a gravel bed; and q_s=sand transport capacity calculated with a transport equation.

In the calculation presented in this paper, it is assumed that

$$k_o = \max(2D_s, 2D_g - \eta) \tag{5}$$

$$k_s = 2D_s \tag{6}$$

in which D_s=geometric mean size for sand; D_g=geometric mean size for gravel; and η=thickness of sand deposit over the gravel bed.

Note that according to Eqs. (5) and (6), $k_o = k_s$ if $\eta \geq 2(D_g - D_s)$, and according to Eq. (4) q_{sr} would be identical to q_s under such conditions. Thus, the proposed roughness correction to calculated sediment transport capacity was applied only when the sand deposit over the gravel bed is very thin.

Correction of Predicted Sand Transport over Gravel Bed due to Partial Area Coverage

For sand transport over a gravel bed, sand covers only the interstices of the surface gravel before it is thick enough to cover the entire gravel bed. Hence, the sand transport capacity calculated with a sand transport equation that assumes the bed is completely covered with sand needs to be corrected for partial area coverage. Here, a simple correction is introduced based on the fact that (1) there is zero sand transport when there is no sand in the bed (i.e., a zero thickness results in zero transport); and (2) no correction is needed when sand covers the entire bed. Assuming a linear relation, the following simple correction is introduced in the DREAM-1 simulations presented in this paper:

$$q_{sa} = \begin{cases} \dfrac{\eta}{2(D_g - D_s)} q_s & \text{for} \quad \eta < 2(D_g - D_s) \\ q_s & \text{for} \quad \eta \geq 2(D_g - D_s) \end{cases} \tag{7}$$

in which q_{sa}=sand transport capacity corrected for partial sand coverage. Note that Eq. (7) is constructed according to the same argument provided in the roughness correction that sand covers the gravel surface when $\eta \geq k_0 - k_s = 2(D_g - D_s)$.

Combining the roughness correction [Eq. (4)] and the partial sand coverage [Eq. (7)] yields

$$q_s' = \begin{cases} \dfrac{\eta}{2(D_g - D_s)} \left(\dfrac{2D_s}{2D_g - \eta}\right)^{7/20} q_s & \text{for} \quad \eta < 2(D_g - D_s) \\ q_s & \text{for} \quad \eta \geq 2(D_g - D_s) \end{cases} \tag{8}$$

in which q_s'=sand transport capacity with both roughness and partial sand coverage corrections. A graphic representation of Eq. (8) is shown in Fig. 5.

References

ACOE. (1993). "HEC-6 scour and deposition in rivers and reservoirs." *User's manual*, ver. 4.1, Hydrologic Engineering Center, ⟨http://www.hec.usace.army.mil/software/legacysoftware/hec6/hec6-documentation.htm⟩ (September 2007).

Bountry, J., and Randle, T. (2001). "Hydraulic and sediment transport analysis and modeling, Appendix B in Savage Rapids Dam Sediment Evaluation Study." *Technical Rep. Prepared by the Dept. of Interior, Bureau of Reclamation*, ⟨http://www.usbr.gov/pn/programs/lcao_misc/pdf/savagerapds/Appendix%20B.pdf⟩ (September 2007).

Brownlie, W. R. (1982). "Prediction of flow depth and sediment discharge in open channels." Ph.D. thesis, California Institute of Technology, Pasadena, Calif.

Chaudhry, M. H. (1993). "Open-channel flow." Prentice-Hall, Englewood Cliffs, N.J.

Cui, Y., Braudrick, C., Dietrich, W. E., Cluer, B., and Parker, G. (2006a). "Dam removal express assessment models (DREAM). Part 2: Sample runs/sensitivity tests." *J. Hydraul. Res.*, 44(3), 308–323.

Cui, Y., and Parker, G. (2005). "Numerical model of sediment pulses and sediment-supply disturbances in mountain rivers." *J. Hydraul. Eng.*, 131(8), 646–656.

Cui, Y., Parker, G., Braudrick, C., Dietrich, W. E., and Cluer, B. (2006b). "Dam removal express assessment models (DREAM). Part 1: Model development and validation." *J. Hydraul. Res.*, 44(3), 291–307.

Cui, Y., Parker, G., and Paola, C. (1996). "Numerical simulation of aggradation and downstream fining." *J. Hydraul. Res.*, 34(2), 185–204.

Cui, Y., Parker, G., Pizzuto, J., and Lisle, T. (2003). "Sediment pulses in mountain rivers. Part 2: Comparison between experiments and numerical predictions." *Water Resour. Res.*, 39(9), 1240.

Cui, Y., and Wilcox, A. (2008). "Chapter 23: Development and application of numerical models of sediment transport associated with dam removal." *Sedimentation engineering: Theory, measurements, modeling, and practice, ASCE manual 110*, M. H. Garcia, ed., ASCE, Reston, Va.

Gomez, B., and Church, M. (1989). "An assessment of bedload sediment transport formulae for gravel-bed rivers." *Water Resour. Res.*, 25(6), 1161–1186.

Goodwin, P. (2004) "Analytical solutions for estimating effective discharge." *J. Hydraul. Eng.*, 130(8), 729–738.

Meyer-Peter, E., and Müller, R. (1948). "Formulas for bed-load transport." *Proc., 2nd Congress Int. Association for Hydraulic Research*, 39–64.

Parker, G. (1990). "Surface-based bedload transport relation for gravel rivers." *J. Hydraul. Res.*, 28(4), 417–436.

Rathburn, S. L., and Wohl, E. E. (2001). "One-dimensional sediment transport modeling of pool recovery along a mountain channel after a reservoir sediment release." *Regul. Rivers: Res. Manage.*, 17, 251–273.